COMBINING GENERATIVE ADVERSARIAL NETWORKS AND FEDERATED LEARNING FOR COVID-19 DETECTION IN EDGE CLOUD COMPUTING

Project turned in to
SRM University, Andhra Pradesh
to partially complete the requirements needed to be awarded a degree of

B.Tech in CSE
School of Engineering & Sciences

submitted by

Diptendu Kumar Jashu(AP22110010369)

Under the Guidance of

Dr. Md. Muzakkir Hussain

CSE Department
SRM- AP
Neerukonda, Mangalgiri, Guntur
Andhra Pradesh - 522 240
May 2024

PROCLAMATION

In order to partially meet the requirements for the award of a Bachelor of Technology degree in the Computer Science & Engineering SRM University-AP I, the undersigned, hereby declare that the project report **Combining Generative Adversarial Networks and Federated Learning for COVID-19 Detection in Edge Cloud Computing** provided is a legitimate work completed by me under the guidance of Dr. Md. Muzakkir Hussain. I am aware that breaking any of the aforementioned will result in disciplinary action from the university and/or the institute. It may also lead to legal action against the sources that were improperly referenced or from whose permission was not sought. No other university's degree has ever been awarded using this report as the foundation.

Place	: SRM University AP	Date	: June 9, 2024
Name of student	: Diptendu Kumar Jashu	Signature	: 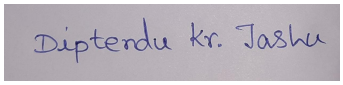

DEPARTMENT OF COMPUTER SCIENCE & ENGINEERING

SRM University-AP

Neerukonda, Mangalgiri, Guntur

Andhra Pradesh - 522 240

Accredited

This certifies the accuracy of the study that Diptendu Kumar Jashu submitted titled **"Combining Generative Adversarial Networks and Federated Learning for COVID-19 Detection in Edge Cloud Computing."**

In partial fulfilment of the requirements for the award of a Master of Technology degree, Marshu has submitted to SRM University-AP a genuine record of the project work completed under our direction and supervision. No other university or institute has received this report, in any format, for any reason.

Project Guide	Head of Department
Name : Dr. Md. Muzakkir Hussain	Name : Prof. HoD Name
Signature:	Signature:

CREDIT

I would like to express my gratitude and debt of gratitude to everyone who assisted me in writing this project report, which is titled **"Combining Federated Learning and Generative Adversarial Networks for COVID-19 Detection in Edge Cloud."**

Compute it and give a good presentation of it.

I would also want to express my gratitude to **Dr. Md. Muza-kkir Hussain**, my supervisor and mentor at the Department of Computer Science & Engineering, for his invaluable advice and crucial contribution throughout the writing of this report. For his encouragement, Prof. HoD Name, Head of the Department of Computer Science & Engineering, is also appreciated.

My classmates have always been supportive, and I appreciate their listening to my presentations about the Project-related work with patience.

Diptendu Kumar Jashu(Reg. No. AP22110010369)
Secoend year - B.Tech - CSE - Section F
CSE Department
SRM AP

SUMMARY

COVID-19 is now considered a dangerous pandemic due to its fast global spread. While the use of artificial intelligence (AI) techniques for COVID-19 detection has grown, privacy concerns have been raised by the fact that many of these techniques rely on sharing data with cloud data centres. This paper presents FedGAN, a unique federated learning (FL) technique that uses edge cloud computing to handle privacy concerns and produce realistic COVID-19 pictures. To recreate the real COVID-19 data distribution, a Generative Adversarial Network (GAN) is first developed here. In this model, each edge-based medical institution trains a generator and a discriminator based on Convolutional Neural Networks (CNNs) locally. Then, a novel FL method is shown, which allows local GANs to cooperate and share learned parameters with a cloud server to improve the capacity of the global GAN model to produce realistic COVID-19 pictures without requiring real-time data sharing. Each hospital institution integrates a differential privacy solution to support privacy in federated COVID-19 data processing. Additionally, a blockchain-based FedGAN architecture that introduces a unique mining technique to minimise running latency and decentralises the FL process is presented to enable safe COVID-19 data analytics. Comparing this strategy to other available techniques for COVID-19 detection, simulation results show how successful it is. COVID-19, edge cloud, federated learning (FL), and generative adversarial network (GAN) are some of the key keywords.

CONTENTS

ACKNOWLEDGMENT i

ABSTRACT ii

Chapter 1. OVERVIEW OF THE PROJECT 1

Chapter 2. MOTIVATION 4

Chapter 3. LITERATURE SURVEY 7

Chapter 4. SYSTEM ARCHITECTURE 10

4.1 Netowrk Architecture 10

4.2 Independent AI Model for Covid disease Identification 12

Chapter 5. FEDGAN MODEL CONCEPTUALISED FOR COVID DETECTION 14

5.1 An Analytical Study of FedGAN 14

5.2 Training of FedGAN for COVID-19 Detection 16

5.3 Unique Security for FedGAN 18

Chapter 6. FEDERATED LEARNING BASED ON BLOCKCHAIN FOR COVID-19 DETEC 19

6.1 Operational Protocol of the FedGAN Based on Blockchain 20

6.2 Suggested Consensus Process for FedGAN Based on Blockchain 22

Chapter 7. RESEARCH AND PERFORMANCE ANALYZATIONS 26

7.1 PERFORMANCE EVALUATIONS AND EXPERIMENTS 26

7.1.1 Experimental Settings 26

7.2 FL and GAN Performance Assessments 29

7.2.1 Evaluation of FedGAN Training 29
7.2.2 Assessing Covid Detection Effectiveness Using FedGAN 33
7.2.3 Assessment of Comparative Privacy-Enabled FedGAN Efficiency 38
7.3 Assessments of FedGAN Performance Using Blockchain 39
7.3.1 Block Verification for the Latency Performance 40
7.3.2 Precision Outcomes 40
7.3.3 The effectiveness of the overall running latency 41

Chapter 8. FINAL THOUGHTS AND NEXT PROJECTS 43
8.1 Concluding Thoughts 43
8.2 Future ideas for our project 43

REFERENCES 45

Chapter 1

OVERVIEW OF THE PROJECT

Within a month following the COVID-19 pandemic's worldwide outbreak, the World Health Organisation (WHO) declared it to be a pandemic due to its severe effects on public health and the world economy. Recently, automated COVID-19 diagnosis and detection utilising X-ray pictures has been achieved with the use of artificial intelligence (AI) techniques such as machine learning (ML) and deep learning (DL). Convolutional neural networks (CNNs), a DL-based technique, have been created to extract critical characteristics from chest X-rays and use them to identify COVID-19 patients. However, compiling a sizable dataset of X-ray images linked to COVID-19 is costly and time-consuming, necessitating the participation of multiple patients and specialists. Furthermore, the potential of infection to medical personnel during the COVID-19 pandemic presents additional hurdles for data gathering.

Through the interaction of a generator and a discriminator in a min-max game, generative adversarial networks (GANs) have lately garnered attention for medical imaging applications. This technology allows for the development of high-quality synthetic pictures from original data. Because GANs provide realistic synthetic data, they reduce the workload associated with data collecting and enhance COVID-19 data training. Nevertheless, in real-world situations, COVID-19 picture collections are dispersed throughout several locations, and the quantity and variety of data at each site are insufficient to properly train a GAN for the full dataset. Furthermore, data

owners, including hospitals, are reluctant to share their data with centralised data centres because to institutional laws and rising privacy concerns, which makes COVID-19 analytics more difficult. It is difficult to compile scattered data on a single server because of this conundrum.

Emerging distributed collaborative AI called federated learning (FL) has potential to help with COVID-19 prediction tasks and other intelligent health data analytics. An aggregator such as a cloud server facilitates collaborative AI training across numerous data sources with FL. By communicating model gradients rather than actual data, each institution may train its data model, preserving data privacy and cutting down on data transmission and storage costs. It is natural to use FL integrated with GANs to build a federated generative model over these distributed institutions, given the distribution of data for generative learning across different medical institutions, such as COVID-19 X-ray images stored in hospitals. This approach addresses important challenges such as dataset limitations, privacy protection, and constrained training performance in COVID-19 analytics.

Still, there are a number of problems with the FL systems in use today. For model aggregation, traditional FL frameworks sometimes rely on a single server, which might result in single-point failures in the event that the server is hacked. Furthermore, because hospitals are required to utilise a central server for data training, hostile assaults on the server may alter or steal model information without permission, or they may take advantage of user information implicitly transmitted by model updates, making FL inaccurate. With its decentralised networking architecture, blockchain technology has shown promise in this regard as a means of coordinating the FL process in lieu of the central server. Hospitals may engage in FL data training decentralised, without relying on a central server, thanks to blockchain

technology. This decentralised strategy greatly lowers the possibility of single-point failures and lessens their dangers.

Chapter 2

MOTIVATION

The inspirations for our work can be clarified as takes after. Firstly, in spite of various investigate endeavors, most existing GAN calculations [15]–[18] for COVID-19 analytics are prepared on restricted and imbalanced datasets from a single institution, which cannot accomplish the specified COVID-19 location precision. Besides, amid a widespread, due to expanding client security concerns and strict controls, therapeutic teach such as clinics are hesitant to share their COVID-19 picture information with a central information center for AI preparing. This requires COVID-19 information preparing without information sharing. Thirdly, the joining of FL and GANs presents a intriguing inquire about course that can improve COVID-19 picture enlargement with protection changes for way better infection discovery and determination. Be that as it may, its potential has not been completely investigated within the COVID-19 detection space within the existing writing [21]–[24]. At last, there's an critical have to be create a unused blockchain arrangement for secure and low-latency combined information preparing to back proficient COVID-19 location amid the widespread.

Propelled by these challenges, we propose a novel conspire called FedGAN for privacy-assured and effective COVID-19 discovery by empowering a joint plan of GAN and FL over therapeutic educate in edge cloud computing. The essential objective of our proposed conspire is to create high-quality manufactured picture information to bolster COVID-19 location errands without requiring the sharing of COVID-19 picture information.

Our arrangement addresses the issues of information impediment and lopsidedness through generative learning, whereas too upgrading COVID-19 information privacy. Additionally, it moves forward COVID-19 discovery execution by leveraging the collaboration of different information sources from dispersed educate. Besides, we present a unused blockchain-based FedGAN system for secure COVID-19 information analytics, decentralizing the FL prepare with a novel mining arrangement for moo running idleness. A comparison of our article with related works based on a few key highlights is summarized in Table I. In outline, the interesting commitments of this article are highlighted as takes after.

1. textbfInnovative FedGAN Approach: We present a spearheading FedGAN scheme for COVID-19 discovery, which combines the qualities of GAN and FL over disseminated restorative educate in edge cloud computing. This show exceeds expectations at creating practical COVID-19 X-ray pictures, in this manner helping programmed COVID-19 discovery in the midst of information shortage at person teach amid the widespread.

2. textbfCollaborative Information Increase Procedure: We propose a collaborative information increase approach where each edge-based institution's GAN, comprising of a discriminator and a generator, trains on the other hand. The prepared parameters are at that point upgraded to a cloud server without uncovering the real picture tests. This arrangement empowers unified GAN preparing to construct a worldwide GAN show that produces synthetic COVID-19 X-ray pictures. To guarantee security in combined COVID-19 information analytics, we coordinated a differential protection arrangement at each clinic institution.

3. textbfSecure Blockchain-Based FedGAN System: We assist propose a blockchain-based FedGAN system for secure COVID-19 information an-

alytics by decentralizing the FL handle over clinic teach. A novel mining component is presented to address the mining idleness caused by blockchain appropriation within the FL framework, an issue not already handled within the writing. Additionally, we investigate the potential of blockchain-based FedGAN in real-world COVID-19 detection scenarios.

4. textbfEffective CNN-Based Classifier: We plan an proficient CNN-based classifier competent of adaptably performing COVID-19 classification into three labeled categories: COVID-19 positive, normal, and pneumonia. Broad recreations are actualized to assess the adequacy of our plans, illustrating noteworthy changes in COVID-19 location with moo running idleness compared to existing strategies.

Chapter 3

LITERATURE SURVEY

A few thinks about utilizing GANs and unified learning (FL) have been proposed for supporting in COVID-19 location assignments. Particularly, Motamed et al. [15] and Khalifa et al. [16] presented GAN-based techniques for distinguishing COVID-19 X-ray pictures, nearby exchange learning for lung division to encourage classification. The think about sketched out in [17] actualized an picture union approach for creating high-quality COVID-19 chest tomography (CT) pictures to bolster profound learning (DL)-based semantic division and classification. Furthermore, [18] investigated the application of conditional GANs for engineered chest X-ray picture enlargement, coming about in quickened COVID-19 discovery with made strides classification execution. The potential of GANs in moderating information confinements amid the COVID-19 widespread was showcased in [19], where DL-based models such as AlexNet, GoogleNet, and ResNet18 were utilized to evaluate engineered information quality and make COVID-19-related forecasts. Another think about [20] utilized GANs for assessing versatility designs amid the COVID-19 widespread inside complex social settings and constrained preparing datasets from different sources.

Moreover, later inquire about has dug into the applications of FL in COVID-19 determination and location. For occurrence, [21] proposed a energetic fusion-based FL approach for demonstrative picture analytics to distinguish COVID-19 cases, emphasizing a client determination instrument based on neighborhood demonstrate exhibitions and a show combination

arrangement for FL conglomeration. The inquire about displayed in [22] presented an FL conspire for combined COVID locale division utilizing chest CT pictures, including collaboration among clinics from China, Italy, and Japan. So also, [23] created a combined DL system for privacy-enhanced location of lung anomalies caused by COVID-19, utilizing CNN models at person teach and conglomerating slopes at a central information center. In addition, Feki et al. [24] utilized FL to build a COVID-19 disease screening conspire based on chest X-ray pictures, exhibiting promising comes about in COVID-19 classification compared to standalone approaches without league. The achievability of FL was advance evaluated through real-world tests in [25] for COVID-19 X-ray picture analytics and classification.

With respect to blockchain-based FL, [26] proposed an FL show coordinates with blockchain for COVID-19 CT imaging in collaboration with different clinics, centering on creating a information normalization-based FL procedure for precisely preparing collaborative profound CNN models utilizing datasets from differing sources. The conceptual integration of blockchain, edge computing, and FL for controlling the COVID-19 widespread was presented in [27], whereas [28] analyzed the potential benefits of coordination blockchain and FL for wellbeing information analytics. Be that as it may, these works [27], [28] needed execution and recreation comes about. Other thinks about [29] and [30] presented blockchain-based FL plans for wellbeing Web of Things (IoT) systems, but their parts in COVID-19 location were not investigated. Works in [31] and [32] moreover proposed blockchain-based FL plans basically to address assault issues in information communication and show accumulation. All things considered, existing writing [26]–[29], [31], [32] has not tended to the idleness challenges postured by blockchain mining in blockchain-FL frameworks. Besides, an

coordinates demonstrate joining blockchain, FL, and GANs, and its examination within the COVID-19 context, remains unexplored within the current writing.

Features	→[21]	[22]	[26]	[27]	[29]	[31]	Ours
FL for COVID-19	✓	✓					✓
Integrated FL-GAN for COVID-19							✓
Differential privacy design					✓		✓
Decentralized FL training			✓			✓	✓
Low-latency blockchain design						✓	✓
Integrated blockchain-FL for COVID-19			✓				✓

Thesis Framework

The ensuing segments of this article are organized as takes after: Area II traces the framework show, specifying the standalone GAN demonstrate as the foundational approach for COVID-19 picture expansion. Taking after this, in Segment III, we present our FedGAN show, which progresses upon COVID-19 picture enlargement by joining security contemplations, at the side showing its hypothetical examination. Furthermore, we present a novel blockchain-based FedGAN system for decentralized COVID-19 information analytics. In Area V, we conduct recreations to evaluate the viability of our approach and compare it with other pertinent techniques. Finally, Area VI gives concluding comments for this article.

Chapter 4

SYSTEM ARCHITECTURE

Here we introduce the Nural network of the suggested strategy and then examines this basic stand-alone method for COVID-19 identification.

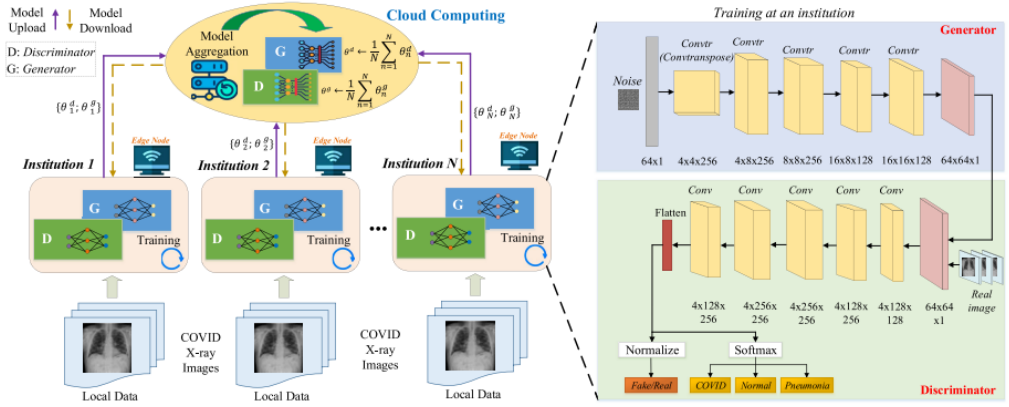

Fig : FedGAN architecture that is suggested for COVID detection.

4.1 NETOWRK ARCHITECTURE

This introduced FedGAN model for Covid detection as demonstrated in above figure. This model includes a group N of many edge nodes are located in hospitals and other healthcare facilities, as well as a cloud server. It's important to remember that these ENs can be local computers or robust IoT devices located in hospitals for data training purposes. Each organisations $n \in N$ participates in the federated learning process by its own Covide X-ray image data to collaboratively develop a global generative adversarial network, assisted by the cloud online server. The objective is to produce high-quality artificial Covid X-ray images to enhance complete detection

accuracy.

Every EN is built with a GAN, which consists of a CNN-based discriminator and generator. Specifically, Every organisation teaches a generator how to distribute generating data p_g^n according to its datasheet D_n, with motive of replicating the real data distribution p_d^n, where $p_g^n = p_d^n$.

This is accomplished by the generator creating a synthetic COVID-19 image data point $G_n(z, \theta_g^n)$, where G_n is the CNN with parameters θ_g^n, using random noise z from a probability distribution $p_z^n(z)$. Furthermore, we construct an additional CNN at each institution to function as a discriminator $D_n(x, \theta_d^n)$ with the objective of differentiating between actual COVID-19 image data points x from the distribution $p_n(x)$ and those produced by the generator. For genuine data x, the discriminator returns 1; for generated data $G_n(z, \theta_g^n)$, it returns 0. In order to trick the discriminator, the generator and discriminator at each hospital work together to optimise the parameters θ_g^n and θ_d^n. This way, the generator generates synthetic data distributions p_g^n that resemble the real data distributions p_d^n. The goal function of the GAN at every institution n may be expressed mathematically as a min-max game with a value function $V_n(D, G)$:

$$\min_G \max_D V_n(D, G) = E_{x \sim p_d^n}[\log D_n(x)] + E_{z \sim p_z^n}[\log(1 - D_n(G_n(z)))] \quad (1)$$

where the probability that D_n classifies x as real data is $D_n(x)$ and the probability that D_n identifies data created by G_n is $D_n(G_n(z))$. The expectation is represented by E. The first term in equation (1) makes sure that the discriminator regulates how closely synthetic samples resemble genuine samples, while the second term penalises the generator for producing unrealistic points. As a result, in equation (1), the generator tries to minimise the value function $V_n(D, G)$ whereas the discriminator D_n tries to maximise it.

4.2 INDEPENDENT AI MODEL FOR COVID DISEASE IDENTIFICATION

In this portion, we look at the standalone GAN, a conventional strategy utilized for COVID-19 discovery. Here, each institution trains the GAN freely utilizing its possess information set without combined learning.

First proposal: When a generator G_n is supplied, the best discriminator is:

$$D_n^* = \frac{p_n^d}{p_n^d + p_n^g} \quad (2)$$

Evidence: For a generator G_n, we may obtain the probability distribution function for the generator p_n^g. Formula (1) allows us to express the value function V_n as follows:

$$V_n(D_n, G_n) = \int_{\mathcal{X}} p_n^d(x) \log D_n(x)\, dx + \int_{\mathcal{Z}} p_n^z(z) \log(1 - D_n(G_n(z)))\, dz = \int_{\mathcal{X}} \left[p_n^d(x) \log D_n(x) + p_n^g(x) \log \right.$$

(3)

We know that the function $a\log(y) + b\log(1-y)$ reaches its minimum value at $\left(\frac{a}{a+b}\right)$ for $y \in (0,1)$, which leads us to the result in equation (2).

Theorem 1: The optimal value of a standalone GAN for COVID-19 detection is:

$$V_n^*(D_n, G_n) = -\log 4 + 2 \times \mathrm{JSD}(p_n^d \| p_n^g) \quad (4)$$

where $\mathrm{JSD}(p_n^d \| p_n^g)$ is the Jensen-Shannon divergence between distributions p_n^d and p_n^g [33].

Evidence: Using (2) and (3), we obtain

$$V_n^*(D,G) = \int_{\mathcal{X}} \left[p_n^d(x) \log D_n^*(x) + p_n^g(x) \log(1 - D_n^*(x)) \right] dx = \int_{\mathcal{X}} \left[p_n^d(x) \log \left(\frac{p_n^d(x)}{p_n^d(x) + p_n^g(x)} \right) + p_n^g(x) \log \right.$$

$$= \int_{\mathcal{X}} \left[p_n^d(x) \log \left(\frac{p_n^d(x)}{\frac{p_n^d(x)+p_n^g(x)}{2} \cdot 2} \right) + p_n^g(x) \log \left(\frac{p_n^g(x)}{\frac{p_n^d(x)+p_n^g(x)}{2} \cdot 2} \right) \right] dx$$

$$= \int_{\mathcal{X}} \left[p_n^d(x) \log \left(\frac{p_n^d(x)}{\frac{p_n^d(x)+p_n^g(x)}{2}} \right) + p_n^g(x) \log \left(\frac{p_n^g(x)}{\frac{p_n^d(x)+p_n^g(x)}{2}} \right) \right] dx - \log 4$$

$$= \int_{\mathcal{X}} \left[p_n^d(x) \log p_n^d(x) + p_n^d(x) \log \frac{2}{p_n^d(x) + p_n^g(x)} + p_n^g(x) \log p_n^g(x) + p_n^g(x) \log \frac{2}{p_n^d(x) + p_n^g(x)} \right] dx - \log 4$$

$$= -\log 4 + \mathrm{KL}\left(p_n^d(x) \middle\| \frac{p_n^d(x) + p_n^g(x)}{2} \right) + \mathrm{KL}\left(p_n^g(x) \middle\| \frac{p_n^d(x) + p_n^g(x)}{2} \right) = -\log 4 + \mathrm{JSD}(p_n^d \| p_n^g)$$

The Kullback-Leibler divergence is denoted by KL. The Jensen-Shannon divergence between probability distributions $A(x)$ and $B(x)$ is known to be $\mathrm{JSD}(A\|B)$, which is defined as follows: $\mathrm{KL}(A\|C) + \mathrm{KL}(B\|C) = 2 \times \mathrm{JSD}(A\|B)$, where $C = \frac{1}{2}(A + B)$. This information is based on [33]. Thus, based on (4), we find

$$V_n^*(D,G) = -\log 4 + 2 \times \mathrm{JSD}(p_n^d \| p_n^g),$$

As $\mathrm{JSD}(p_n^d \| p_n^g)$ is consistently nonnegative [33], $-\log 4$ is the global minimum of $V_n^*(D,G)$ in the standalone GAN-based COVID-19 detection. We will introduce the suggested FedGAN and demonstrate its theoretical benefits in GAN training for effective COVID-19 identification in the sections that follow.

Chapter 5

FEDGAN MODEL CONCEPTUALISED FOR COVID DETECTION

5.1 AN ANALYTICAL STUDY OF FEDGAN

The value function in FedGAN is expressed as a multi-agent game whereby generators and discriminators from every institution denoted by $n \in \mathcal{N}$ participate. The generators work together to create phoney COVID-19 X-ray pictures that fool discriminators from different universities, while the discriminators try to differentiate between the fake images and the actual data. This cooperative interaction between generators and discriminators therefore characterises the FedGAN value function.

$$V^{\text{fed}}(D, G) = \sum_{n=1}^{N} V_n(D_n, G_n)$$

$$= \sum_{n=1}^{N} \left[E_{X \sim p_d} \log D_n(x) + E_{\sim p_g} \log(1 - D_n(G(z))) \right] \quad (6)$$

Furthermore, the optimal discriminator D_n for FedGAN, given any generators G_n, closely resembles that of the standalone GAN, as described in equation (2). Thus, it is possible to calculate the ideal FedGAN value for COVID-19 detection in a comparable way.

$$
\begin{aligned}
V_n^{\text{bce}}(D,G) &= \sum_{n=1}^{N} \int \left[p_n^d(x) \log D_n^*(x) + p_n^g(x) \log(1 - D_n^*(x)) \right] dx \\
&= \sum_{n=1}^{N} \int \left[p_n^d(x) \right. \\
&\quad \left. \log\left(\frac{p_n^d(x)}{p_n^d(x)+p_n^g(x)} \right) + p_n^g(x) \log\left(\frac{p_n^g}{p_n^d+p_n^g} \right) \right] dx \\
&= \sum_{n=1}^{N} \int \left[p_n^d(x) \log\left(\frac{p_n^d(x)}{2p_n^d(x)+p_n^g(x)} \right) + p_n^g(x) \log\left(\frac{p_n^g(x)}{2p_n^d(x)+p_n^g(x)} \right) \right] dx \\
&= \sum_{n=1}^{N} \left[-\log 4 + 2 \times \text{JSD}(p_n^d \| p_n^*) \right] \\
&= \text{-nlog}\,4 + 2 \times \sum_{n=1}^{N} \text{JSD}(p_n^d \| p_n^*). \quad (7)
\end{aligned}
$$

The generators at each institution n in the multi-agent game scenario are trained to precisely represent the features of the real data distribution p_{d_n}, where $p_{d_n} = p_{g_n}$ for $n \in \mathcal{N}$ can achieve the minimum of the value function $V_{\text{fed}}(D,G)$ when $p_{d_n} = p_{g_n}$ can be reached. As a result, the solution to equation (7) suggests that the Jensen-Shannon divergences added together between each generator distribution and itself, p_{g_n}, equal zero. Consequently, $V_{\text{fed}}^*(D,G) = -n \log 4$ can be the best value function for FedGAN. According to this investigation, the federated method outperforms the standalone method in achieving the GAN value function's global minimum. This is made possible by the cooperation of several institutions, which allows for the learning of the distribution of data throughout the population. Put differently, the suggested FedGAN method can learn the COVID-19 picture distribution more successfully, leading to the production of superior synthetic image data that makes detection jobs easier. There will be comprehensive simulations carried out to confirm this benefit.

5.2 TRAINING OF FEDGAN FOR COVID-19 DETECTION

In each global round, each institution $n \in \mathcal{N}$ updates the discriminator and generator parameters $\theta_{d_n,t}$ and $\theta_{g_n,t}$ and exchanges them with the cloud server for aggregation. This is done as part of the FedGAN training process. It is presumed that the image data of COVID-19 are dispersed independently and uniformly (iid) across various institutions. All institutions jointly train their generator (G_n and discriminator (D_n throughout every global epoch t. In the noise distribution $p_{z_n}(z)$, the generator generates K minibatches of fictitious samples, whereas the discriminator takes samples of K real data from the corresponding image distribution $p_{d_n}(z)$. Next, every organisation changes its discriminator D_n in unison by refining its ascent of the stochastic gradient.

$$\nabla_{\theta_d} \frac{1}{k} \left[\sum_{j=1}^{k} \log D(x^{(j)}) + \log(1 - D(G(z^{(j)}))) \right] \quad (8)$$

$$\nabla_{\theta_g} \frac{1}{k} \sum_{j=1}^{k} \log\left(1 - D\left(G\left(z^{(j)}\right)\right)\right) \quad (9)$$

Training Procedure of the Proposed FedGAN:

Cloud server executes:

Initialize global training period T, local training epoch L, local weights $\theta_n^d, \theta_n^g, \forall n \in \mathcal{N}$, learning rate σ

each global round $t = 1, 2, \ldots, T$

each institution $n \in \mathcal{N}$

$\theta_{n,t+1}^d, \theta_{n,t+1}^g \leftarrow \text{LocalUpdate}(n, \theta_t^d, \theta_t^g)$

$\theta_{t+1}^d \leftarrow \frac{1}{N} \sum_{n=1}^{N} \theta_{n,t+1}^d$

$\theta_{t+1}^g \leftarrow \frac{1}{N} \sum_{n=1}^{N} \theta_{n,t+1}^g$

LocalUpdaten, θ^d, θ^g Run at each institution n

each local epoch $i = 1, 2, \ldots, L$

Sample k minibatchs of noise samples $\{z^{(1)}, z^{(2)}, ..., z^{(k)}\}$ from distribution $p_n^z(z)$

Sample k minibatchs of real data $\{x^{(1)}, x^{(2)}, ..., x^{(k)}\}$ from actual COVID-19 image distribution $p_n^d(x)$

Update the discriminator via (8)

Update the generator via (9)

Update the weights θ^d and θ^g

$\theta^d \leftarrow \theta^d - \sigma \nabla_{\theta^d} \mathcal{L}$

(θ^d, θ^g); $\theta^g \leftarrow \theta^g - \sigma \nabla_{\theta^g} \mathcal{L}(\theta^d, \theta^g)$ (10)

Return θ^d, θ^g to the cloud server

Each institution uploads its revised local weights, θ_n^d and θ_n^g, to the cloud server for model aggregation after finishing the training. The local model parameters, $\theta^d \leftarrow \frac{1}{N} \sum_{n=1}^{N} \theta_n^d$ and $\theta^g \leftarrow \frac{1}{N} \sum_{n=1}^{N} \theta_n^g$, are aggregated by the cloud server using the well-liked model averaging approach. Then, during the upcoming GAN training cycle, these updated global parameters, θ^d and θ^g, are broadcast back to all institutions. The global loss function iteratively converges to the required accuracy across the course of this FedGAN procedure. Algorithm 1 provides specifics on the FedGAN's planned training process.

Since the cloud server in FedGAN just collects parameters—which requires little computer power—each institution bears the majority of the computational load. At the institutional level, we examine the computational complexity. Every institution works together to train its generator and discriminator to update θ_n^g and θ_n^d during each global training cycle. While the discriminator D_n samples k minibatches of actual data with batch size b^d, the generator G_n creates k minibatches of fictitious

samples with batch size b^g.

In order to produce a false data sample, the generator needs to do $kb^g G_{fp}$ floating point operations. Additionally, it needs to have a memory of $kb^g G_{neu}$, where G_{neu} represents the number of generator neurons. That means that $O(kb^g G_{fp} + kb^g G_{neu}) = O(kb^g(G_{fp} + G_{neu}))$ is the generator's computational complexity. Similarly, the computational complexity of the discriminator is $O(kb^d(D_{fp} + D_{neu}))$, where D_{fp} and D_{neu} are the number of neurons required to create a real data sample and the floating point operations, respectively. Thus, for T global training rounds, the total computational complexity at each institution is

$$O(Tk[b^g(G_{fp} + G_{neu}) + b^d(D_{fp} + D_{neu})]).$$

5.3 UNIQUE SECURITY FOR FEDGAN

We incorporate an e-differential privacy approach at each hospital site to further improve privacy for FedGAN training, where e is the discernible bound of all outputs on two neighbouring data sets D and D′ in a database. If e-differential privacy is achieved by a randomised function A, then:

Pr[A(D) S] e^e Pr[A(D′) S] (11)

S falls inside range (A). We use a gradient perturbation approach here with differentially private stochastic gradient descent (DP-SGD) [12], whereby Gaussian noises are introduced to the training, to ensure e-differential privacy. Consequently, the gradient decline update during training round t may be found as follows:

$$_{t+1} =_t -(f(x_t;_t) + c) \quad (12)$$

Where c is the noise that ensures differential privacy and f is the GAN's loss function.

Chapter 6

FEDERATED LEARNING BASED ON BLOCKCHAIN FOR COVID-19 DETECTION

Addressing security concerns related to information leakage and single-point failures is crucial for improved privacy COVID-19 analytics for data particularly with regards the potential threats posed by malicious cloud third parties and centralized FL frameworks. Traditional FL setups, reliant on a single cloud server for aggregation, are susceptible to unauthorized exploitation of hospital data and attacks aimed at intercepting or altering FL updates during aggregation. Moreover, the centralized nature of these systems poses risks of single-point failures, potentially disrupting the entire FL process if the cloud server is compromised. In our later ponder [34], we investigated the part of blockchain in guaranteeing secure Analytics for COVID-19 information. Blockchain innovation empowers decentralized information learning among geologically scattered associations, doing absent with the necessity for a central server. In this setting, we propose a decentralized FedGAN system coordinates with blockchain, as portrayed in Figure 2. By supplanting the centralized cloud server with blockchain, we decentralize the FL conglomeration handle to upgrade security. Furthermore, blockchain upgrades the possibility of applying FL in large-scale healthcare systems by means of encouraging peer-to-peer preparing of picture datasets among interconnected ENs and clinics.

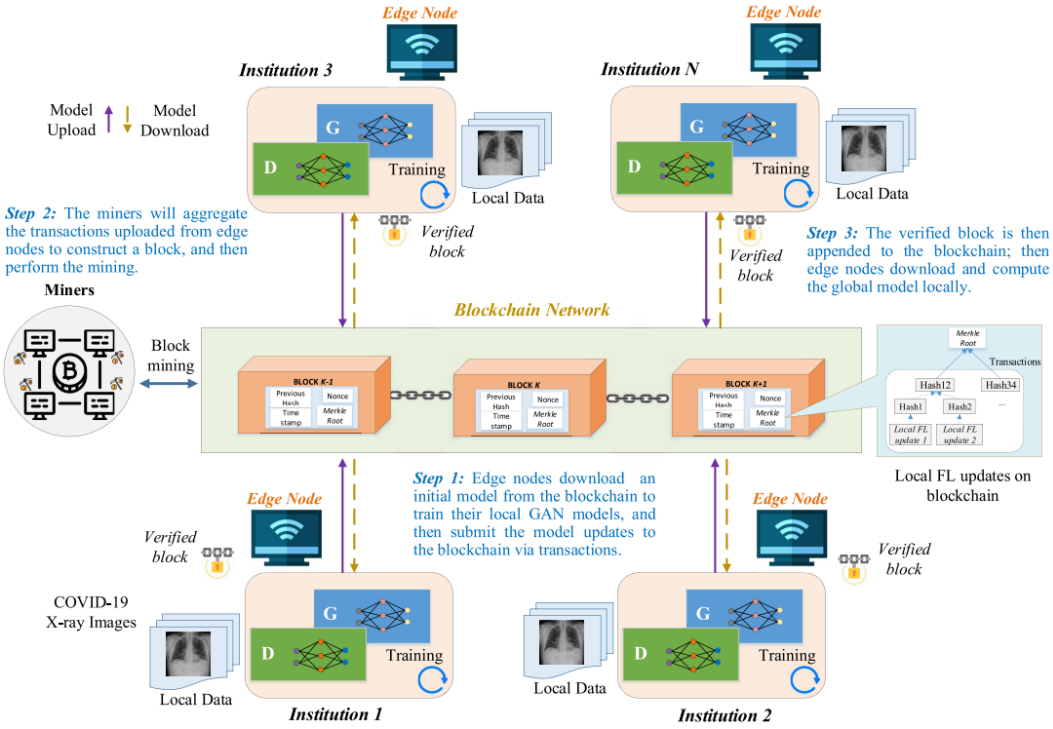

6.1 OPERATIONAL PROTOCOL OF THE FEDGAN BASED ON BLOCKCHAIN

Our FedGAN framework's operational process, which is built on blockchain can be delineated through the following steps:

1. **Joining the Federated Learning Process and Setting Up Wallet Accounts:**

   ENs wishing to share within the FL prepare recover an introductory demonstrate from the blockchain. Each EN moreover sets up a wallet account comprising a open key for distinguishing proof and a private key for exchange marking.

2. **Local Training and Model Update Submission with Differential Privacy:**

   ENs exclusively conduct GAN show preparing, including a generator

and discriminator, utilizing their particular nearby COVID-19 X-ray picture datasets. In case utilizing differential protection, a certain sum of ϵ-differential protection commotion is joined into the slope amid preparing. Taking after neighborhood preparing, ENs yield their show upgrades to the blockchain by creating a exchange.

3. **Transaction Aggregation and Block Verification by Miners:**
   Diggers amalgamate the exchanges from ENs over a assigned period to build a square. In this way, mineworkers lock in in mining to verify the piece utilizing a agreement instrument.

4. **Decentralized Global Model Construction and GAN Training Process:**
   Upon fruitful mining, in case all diggers reach a agreement on the approved square, it is added to the blockchain. ENs can at that point download the piece containing all FL upgrades from other ENs to compute the worldwide demonstrate locally, veering from the conventional FL engineering where the worldwide demonstrate is developed centrally on a cloud server. The GAN preparing cycle proceeds until the specified precision execution is achieved.

This operational strategy explains that the essential idleness costs of blockchain-based FedGAN preparing basically stem from FedGAN preparing idleness and blockchain mining idleness. In this setting, our center lies on moderating blockchain mining inactivity through the presentation of a novel square agreement instrument, as expounded within the ensuing area.

6.2 SUGGESTED CONSENSUS PROCESS FOR FEDGAN BASED ON BLOCKCHAIN

Within the blockchain-based FedGAN framework, as the volume of exchanges (e.g., nearby GAN overhauls) submitted to the blockchain increments, the workload for accomplishing agreement to approve and consolidate these exchanges into the blockchain too heightens altogether. Whereas agreement components like designated Confirmation of Stake (DPoS) have been utilized to supplant computationally seriously agreement plans like Verification of Work, they still involve tall inactivity costs. In existing agreement calculations such as DPoS [36], each mineworker must lock in with a larger part of the entire hubs within the digger gather, in this manner intensifying inactivity and blocking the adaptability of the blockchain framework. Moreover, each digger hub must execute a dreary confirmation prepare over the mineworker arrange, coming about in pointless agreement idleness. In spite of the fact that diminishing the number of mineworker hubs seem relieve agreement idleness, it may compromise blockchain security due to the increased hazard of counting compromised exchanges from malevolent hubs [36]. To address these mining issues, we present a novel lightweight agreement instrument named Confirmation of Notoriety (PoR) for our blockchain-FedGAN framework. In differentiate to the DPoS scheme, we significantly improve digger choice based on a notoriety score assessment approach. Moreover, rather than utilizing rehashed confirmation among mineworker hubs, we actualize a lightweight block confirmation arrangement wherein each mineworker confirms as it were once with another hub amid the agreement prepare, essentially decreasing confirmation idleness. Our PoR agreement comprises of two essential

components: digger hub choice and piece confirmation.

Choice of Miner Node

In this arrange, ENs at first compute the notoriety scores of diggers and after that select the digger hubs to conduct the mining handle.

Calculating Reputation: In our blockchain-based FedGAN framework, other than COVID-19 information preparing, ENs too share within the assign determination strategy to cast votes for mining candidates mindful for blockchain agreement. Each EN casts votes for its favored diggers having the most noteworthy notoriety. Here, a miner's notoriety is gaged by its computational capacity for square mining. Basically, mineworkers distributing more computational assets to mining assignments gather higher notoriety scores, in this way picking up priority in square mining. To realize this, we characterize a notoriety work to evaluate the score for each mineworker as takes after:

Miner Selection: Leveraging the computed notoriety scores, each EN casts votes for mineworker candidates concurring to their positioning in terms of notoriety. The beat mineworkers within the mining bunch with the most elevated notoriety scores are chosen to serve as genuine mineworkers, named as edge diggers (EMs), capable for executing the mining prepare. Moreover, associated to the conventional DPoS system [37], each EM moreover capacities as a square supervisor. This involves errands such as square era, broadcasting squares to other mineworkers for confirmation, and square accumulation taking after confirmation, amid its designated time opening within the agreement prepare.

Simple Block Verification

At first, the square supervisor produces an unconfirmed square enveloping various wellbeing exchanges totaled inside a particular time outline, which is at that point dispersed to all edge diggers (EMs) for confirmation. Veering from the conventional DPoS plot, which depends on dreary confirmation among mineworkers, we present a lightweight Verification of Notoriety (PoR)-based confirmation arrangement. This arrangement empowers each digger to experience confirmation as it were once with another hub amid the agreement handle, subsequently considerably diminishing confirmation idleness.

Each of the K transaction pieces Tr_k ($k = 1, \ldots, K$) that make up the block B—which contains all transactions—is assigned to a specific EM member (EM_m) in the miner group by the block manager. Furthermore, a distinct random number R_m is assigned to every miner EM_m. Then EM_m chooses any miner s ($s \neq n$) to verify its assigned transaction component Tr_k. In case a majority of EMs (minimum 51%) confirm favourable results, the block manager will proceed to the subsequent phase.

Verification of Block Latency

We examine the verification delay related to mining operations in this section. We assume that a transaction component Tr_k is sent to every edge miner (EM). Furthermore, each EM agrees to provide their resources (measured in CPU cycles/s) $C = \{c_1, c_2, \ldots, c_m\}$ to carry out the transaction component k. Each EM n that uses a CPU resource to validate a transaction k is represented by the symbol ϕ_m. Moreover, the size of the verified transaction result Tr_k is represented by Trrek.

In our proposed Proof of Reputation mechanism at an EM, the block

verification process consists of four main steps:

1. transfer of the unconfirmed block from the EMs to the block manager;
2. local confirmation at the EM of the block;
3. providing two EMs with the verification result;
4. The management receives feedback on the verification result from the EMs.

The following formula may be used to determine the delay caused by carrying out these processes at each miner n:

$$\mathrm{T}_m^k = \frac{T_s^k}{c_m} + \epsilon\sigma T_e^4 + \frac{T_r^k}{c_m},\ k \in [1, \ldots, K] \quad (14)$$

In the mean time, within the DPoS model [38], each digger has to perform rehashed confirmation on the complete square B, where its confirmation inactivity is computed as [38]

$$\tau_m^{DRS} = \frac{B}{c_f} + \frac{B^{q+1}}{c_q} + \epsilon\beta|z^q| + \frac{B^r}{c_r} \quad (15)$$

In relation to the whole budget cB_m, B_m denotes the CPU resources needed to execute the block B. Furthermore, the size of the verified result for block B is shown by Bre. All miners n take part in the repeated block verification, as shown by the notation $|LN|$. When comparing equations (14) and (15) for the same block size and number of miners, it is clear that the suggested PoR strategy takes less time to verify than the conventional DPoS scheme. The benefits of our suggested PoR method will be shown in the section that follows.

Chapter 7

RESEARCH AND PERFORMANCE ANALYZATIONS

7.1 PERFORMANCE EVALUATIONS AND EXPERIMENTS

7.1.1 Experimental Settings

For our recreations, we utilize two broadly utilized COVID-19 X-ray information sets: the DarkCOVID information set [7], which contains 620 add up to X-ray pictures, and the ChestCOVID information set [39], which contains 950 add up to X-ray pictures for three classes: COVID-19, ordinary (no pneumonia), and pneumonia (with no COVID-19 contamination). These information sets were assembled from different districts, making them fitting for our FedGAN setting. We part each dataset into preparing and testing sets in an 80: 20 proportion.

As seen in Fig. 1, we built up five educate, each of which contains a generator and a discriminator based on CNNs. With the minibatch set to 32, each discriminator D gets $64 \times 64 \times 1$ COVID-19 X-ray pictures. The discriminator is set up with five covered up layers, each with dropout and LeakyRELU in 128 measurements. In addition, 64-D commotion tests from a commonplace Gaussian dispersion are utilized by each generator G. Each generator comprises five covered up layers, the last mentioned two of which have 128 measurements and the primary three of which have 256 measurements. Preparatory test discoveries are utilized to decide these parameters. Each nearby GAN is prepared for 20 ages amid the 500

worldwide rounds of preparing for the FedGAN.

Moreover, we make a CNN-based classifier with three classes for COVID-19 location: Pneumonia; 2) typical; and 3) COVID-19 positive. An input layer of $32 \times 32 \times 3$ and three covered up convoluted layers highlighting part measurements of 3×3, ReLU actuation capacities, and max pooling contain the CNN engineering. Relu is the enactment in each of the two covered up layers in this case; the primary covered up layer has 32 measurements, whereas the moment layer has 128 measurements. With SGD acting as the optimizer and a softmax work acting as the actuation to supply expectation comes about over three classes, the ultimate layer has three measurements. In expansion, dropout (0.5) and group standardization are connected to anticipate overfitting on the preparing set. A preparing rate of 0.001 is connected to the CNN classifier. Several preparing trials are utilized to select these hyperparameters in arrange to induce exact classification comes about. Each recreation was run utilizing Pytorch on

a desktop server utilizing CUDA 8.0, Nvidia Pascal Titan X, and an Intel Center i9 4.8 GHz CPU with 64 GB of Smash.

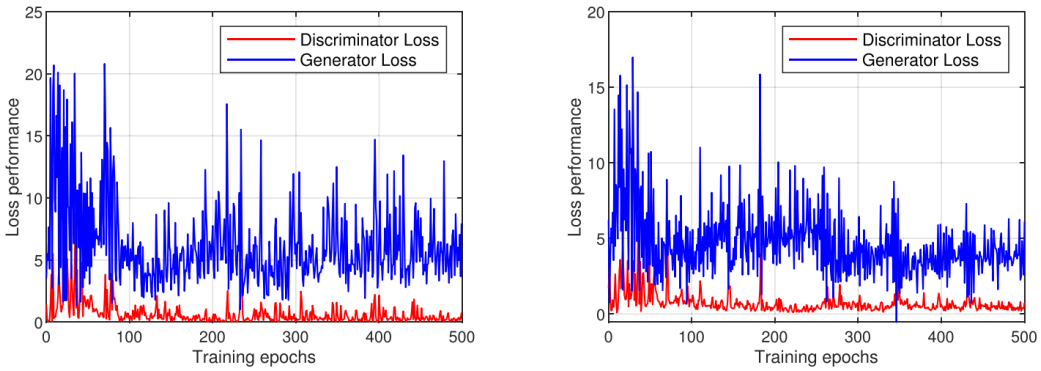

(a) (b)

Analysing the loss of training. (a)FedGAN's loss on the Dark Covid training dataset (b) FedGAN failure on the Chest Covid training

dataset

.

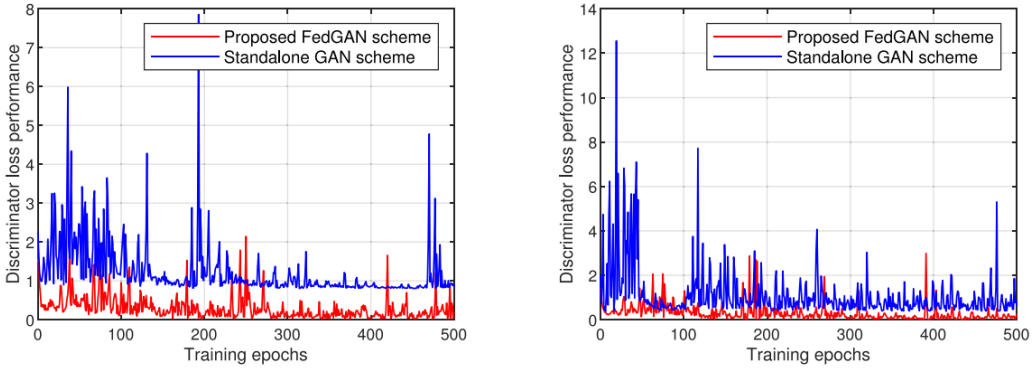

(a) (b)

Discriminator losses are compared. (a) The Dark Covid training data set results in discriminator losses. (b) Discriminator fails during Chest Covid training.

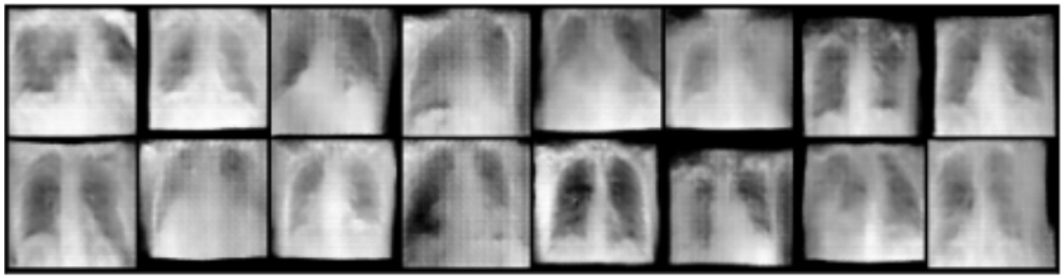

(a)

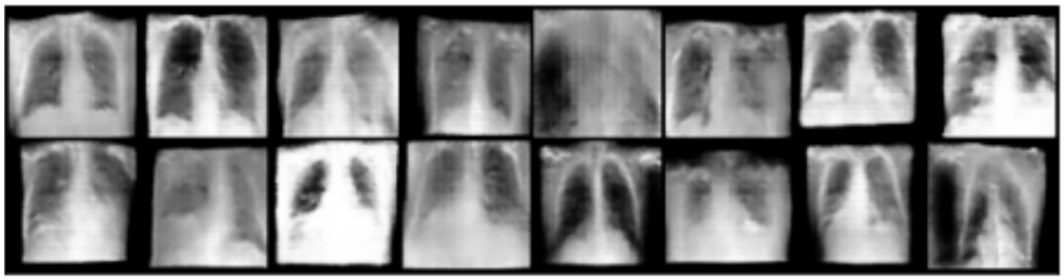

(b)

The Fake Covid X-ray images produced by our FedGAN technic exhibit significantly higher quality compared to those generated by the standalone scheme. (a) Fake Covid X-ray images created using the standalone GAN

scheme. (b) Fake Covid X-ray images created using the proposed FedGAN scheme.

7.2 FL AND GAN PERFORMANCE ASSESSMENTS

We look at the adequacy of our proposed FedGAN conspire and compare it with cutting-edge plans, such as the centralised plot (where all information sets are sent to the cloud for classification), the standalone conspire [5], the standalone plot with GAN [18], the FL conspire without GAN [24], and the standalone conspire with GAN [18]. A CNN-based classifier is utilized by all procedures beneath thought to evaluate COVID-19 location. The displayed discoveries are an normal of five runs of numerical recreations for a reliable assessment.

7.2.1 Evaluation of FedGAN Training

we to begin with survey the FedGAN model's preparing misfortune, which incorporates the discriminator and generator misfortunes for preparing on the DarkCOVID and ChestCOVID information sets over 500 ages. Outstandingly, after 100 ages for both information sets, the discriminator misfortune comes to a steady joining, illustrating that the FedGAN show can orchestrate COVID-19 picture information which the quality of the incorporated information moves forward with preparing. Put something else, the FedGAN demonstrate is able to create high-quality engineered Covid X-ray pictures in such a way that the discriminator is incapable to recognize them from the honest to goodness ones by learning the characteristics of the genuine Covid X-ray pictures.

The discriminator misfortune of the solo GAN strategy [18] and the recommended FedGAN conspire are differentiated in Fig. 4. It is obvious

that the stand-alone arrange is incapable to supply a not too bad outcome in both situations as a result of not having access to the entire data set. On the other hand, because our FedGAN strategy can learn data throughout the whole distribution of all institutions, it can achieve superior minimum loss. The outcomes of these simulations also match our Section III theoretical analysis. Thus, as shown in Fig. 5, our model is able to generate superior COVID-19 X-ray pictures. Table II provides the specifics of how the two data sets' synthetic COVID-19 X-ray image numbers were generated.In this instance, we create 2400 synthetic ChestCOVID photos and 1500 synthetic DarkCOVID images, with the same image volume in each class, addressing imbalance and restriction of the data set. In the upcoming simulations, we will utilise these fake data linked to actual data to discover COVID-19.

	Covid	Normal	Pneumonia
Covid	0.88	0.07	0.06
Normal	0.00	1.00	0.00
Pneumonia	0.02	0.54	0.46

(a)

	Covid	Normal	Pneumonia
Covid	0.94	0.08	0.00
Normal	0.00	1.00	0.00
Pneumonia	0.02	0.13	0.87

(b)

	Covid-19	Normal	Pneumonia
Covid-19	0.96	0.01	0.03
Normal	0.00	1.00	0.00
Pneumonia	0.00	0.21	0.79

(c)

	Covid-19	Normal	Pneumonia
Covid-19	0.99	0.00	0.02
Normal	0.00	0.99	0.00
Pneumonia	0.00	0.16	0.86

(d)

Fig : Disarray frameworks of distinctive plans for Covid location on Chest covid information set. (a) Standalone conspire without GAN. (b) Standalone conspire with GAN. (c) FL plot without GAN. (d) Proposed FedGAN conspire.

result in both circumstances as a result of not having get to to the complete information set. On the other hand, since our FedGAN technique can learn information all through the entire dissemination of all educate, it can accomplish 30 predominant least misfortune. The results of these recreations moreover coordinate our Area III hypothetical examination. In this way, as appeared in Fig. 5, our demonstrate is able to create prevalent COVID-19 X-ray pictures. Table II gives the specifics of how the two information sets' engineered COVID-19 X-ray picture numbers were generated.In this occurrence, we make 2400 engineered ChestCOVID photographs and 1500 manufactured DarkCOVID pictures, with the same picture volume in each course, tending to imbalance and restriction of the information set. Within the up and coming recreations, we are going use these fake information

	Covid-19	Normal	Pneumonia
Covid-19	0.87	0.06	0.07
Normal	0.00	1.00	0.00
Pneumonia	0.01	0.55	0.45

(a)

	Covid-19	Normal	Pneumonia
Covid-19	0.93	0.07	0.00
Normal	0.00	1.00	0.00
Pneumonia	0.02	0.11	0.86

(b)

	Covid-19	Normal	Pneumonia
Covid-19	0.97	0.02	0.01
Normal	0.00	1.00	0.00
Pneumonia	0.00	0.20	0.80

(c)

	Covid-19	Normal	Pneumonia
Covid-19	0.99	0.00	0.01
Normal	0.00	0.99	0.00
Pneumonia	0.00	0.14	0.85

(d)

Fig : perplexity frameworks of diverse plans for COVID-19 discovery on ChestCOVID information set. (a) Standalone plot without GAN. (b) Standalone plot with GAN. (c) FL plot without GAN. (d) Proposed FedGAN conspire

Dataset	Classes	Original data	Synthetic data
DarkCOVID dataset	COVID-19	150	500
	Normal	232	500
	Pneumonia	238	500
	Sum	**620**	**1500**
ChestCOVID dataset	COVID-19	223	800
	Normal	421	800
	Pneumonia	306	800
	Sum	**950**	**2400**

7.2.2 Assessing Covid Detection Effectiveness Using FedGAN

Determining how much artificial data to utilise for optimum detection ratio is a crucial step in implementing COVID-19 detection. To achieve this, we combine real data and synthetic data based on various ratios, which represents the Dark Covid and Chest Covid data sets, as the number of artificial data divided by the quantity of real data. It is implied that only real data are utilised for training when = 0 and $\beta = 0$. According to Table III, the CNN classifier's accuracy rises with an increase in the mixing ratio . usually rise on the training DarkCOVID subgroups, demonstrating the value of GANs' provided data augmentation for COVID-19 classification. Remarkably, $\alpha = 3$ produces the most

Table 3: CNN Classifier's Precision on Blended Genuine and Manufactured Information on Dark Covid Information Set Table IV: CNN Classifier Precision on Blended Genuine and Engineered Information for Chest covid Information SET precision within the lion's share of preparing Dark Covid sets; in any case, since of the overfitting issue, including more engineered information may break down the exactness execution. In a comparative vein, we too look at the Chest Covid information set in Table IV, which illustrates that $\alpha = 4$ yields the finest precision execution. Subsequently, these blending proportions will be connected to the remaining

reenactments. Following, we survey COVID-19 detection's adequacy. through broadly utilized quality criteria, such as F1-score, affectability, and exactness. Our recommended FedGAN strategy performs way better than elective systems on three measures, as appeared in Table V. For illustration, compared to poorer comes about at other plans, our strategy may raise the exactness and F1 score up to 0.993 and 0.991 for the COVID course within the Chest Covid information set. The benefits of utilizing our FedGAN for COVID recognizable proof are encourage approved by the disarray frameworks in Following figures.

Accuracy of Convolutional Nural Network Classifier on Dark Covid Data Set with Mixed Real and Artificial Data

Training size	$\alpha = 0$	$\alpha = 1$	$\alpha = 2$	$\boldsymbol{\alpha=3}$	$\alpha = 4$
500	0.487	0.550	0.842	**0.911**	0.901
1000	0522	0.614	0.850	**0.925**	0.934
1500	0.663	0.749	0.871	**0.931**	0.927
2000	0.784	0.799	0.872	**0.967**	0.955

Accuracy of Convolutional Nural Network Classifier on Mixed Actual Data and artificial Data on Chest Covid Data

Training size	$\beta = 0$	$\beta = 1$	$\beta = 2$	$\beta = 3$	$\boldsymbol{\beta=4}$	$\beta = 5$
500	0.561	0.617	0.715	0.890	**0.931**	0.900
1000	0.547	0.621	0.745	0.846	**0.945**	0.918
1500	0.57	0.732	0.870	0.871	**0.950**	0.925
2000	0.61	0.808	0.904	0.932	**0.962**	0.953
2500	0.690	0.893	0.945	0.945	**0.973**	0.932

Additionally, we compare several approaches using scores from the fully convolutional semantic segmentation network (FCN). They serve as a gauge for the produced photographs' quality.
on an input segmentation map, which may be put into practice by supplying the FCN with produced X-ray pictures. To assess FCN scores,

we employ three conventional segmentation measures, namely the mean class Intersection-Over-Union (IOU), the per-pixel accuracy, and the perclass accuracy, as per CycleGAN [40]. For both data sets, our FedGAN strategy performs better than the alternative methods, as shown in Table VI. For instance, our technique may raise the per-class accuracy by 29% and the per-pixel accuracy by 29% when the Dark data set was being trained. Compared to the FL scheme without GAN, accuracy increased by 18% and the mean IOU by 12%.Table VII's training of the Chest Covid data demonstrates the gains in FCN scores of our proposed technique over current approaches, indicating the improved stability of image-label translation.

Next, we examine the accuracy of several FL schemes and our FedGAN method in terms of detection performance using test data sets. The independent plan is employed as the because there is no federation.

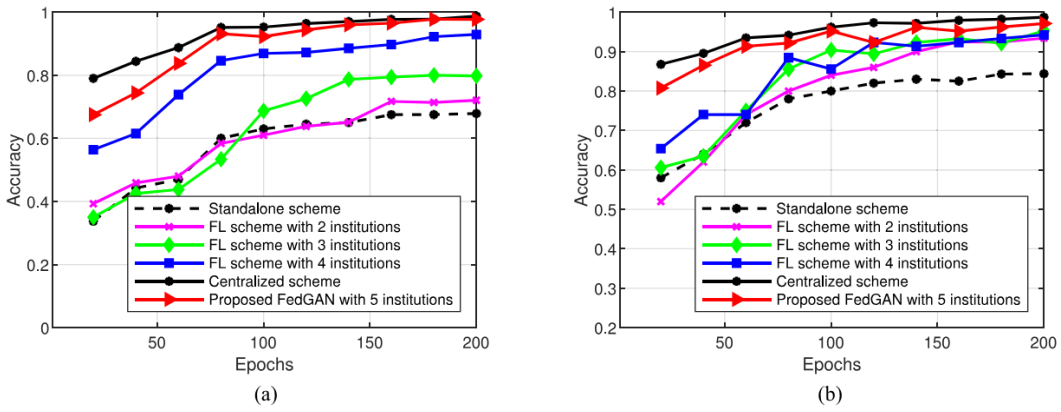

fig : Comparison of accuracy results using various FL systems. (a) COVID detection accuracy on the testing Dark Covid data set. (b) COVID detection accuracy on evaluating the Chest Covid data set .

Next, we examine the accuracy of several FL schemes and our FedGAN method in terms of detection performance using test data sets. Because there is no federation, FCN Score Comparison on Chestcovid Data Set

baseline should have the lowest accuracy rates. The greater the accuracy attained for both data sets, as seen in previous figure ,the greater the number of organisation taking part in the data-driven instruction. This may be explained by the increased efficacy of learning image features due to the utilisation of many data sources, which enhances the in general applicability of the CNN model increases with the number of organisation. On the other hand, our FedGAN scheme is near the centralised system with the whole data set and obtains the best accuracy among other FL techniques. For instance, the accuracy of our scheme is 0.992 for the testing of Dark Covid data when the epoch is 200. This is 8%, 19%, 25%, and 28% greater than the accuracy of the solo scheme and the FL schemes with other organisations.

Comparison of FCN Scores on DarkCOVID Data Set

Schemes	Per-pixel acc.	Per-class acc.	Mean IOU
Standalone scheme without GAN	0.32	0.24	0.28
Standalone scheme with GAN	0.47	0.41	0.35
FL scheme without GAN	0.63	0.52	0.49
Proposed scheme FedGAN	**0.82**	**0.65**	**0.56**

Comparison of FCN Scores on ChestCOVID Data Set

Schemes	Per-pixel acc.	Per-class acc.	Mean IOU
Standalone scheme without GAN	0.45	0.40	0.34
Standalone scheme with GAN	0.59	0.58	0.39
FL scheme without GAN	0.75	0.63	0.43
Proposed scheme FedGAN	**0.87**	**0.74**	**0.59**

Additionally, as shown in Fig. 9, we contrast our scheme's accuracy performance with that of previous COVID-19 detection techniques. Because of its GAN and FL, our FedGAN system can greatly increase the accuracy rate in both data sets.

blend. In other words, following 200 evaluation epochs of the Dark Covid data , our scheme produces greatest accuracy of 0.963 in contrast to our system with GAN (0.856), this scheme without GAN (0.705), and the FL technique without GAN (0.922). Its performance (0.969) is also quite

comparable to the centralised scheme's. Comparable outcomes are also found while analysing the Chest Covid data set., where our suggested FedGAN technique achieves a noteworthy accuracy performance of 0.975. These simulation results show how confidently and successfully our approach can identify COVID-19.

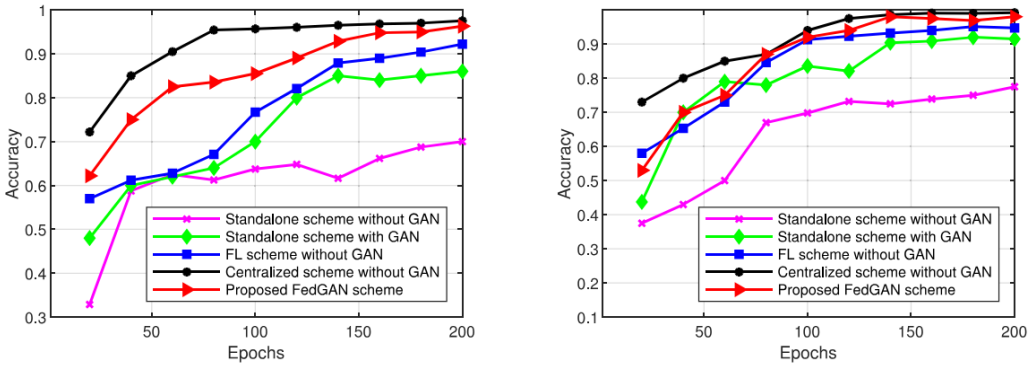

Fig : Accuracy performance comparisons using various Covid dieses detection strategies. (a) Covid detection accuracy on the testing Dark Covid data . (b) Covid detection accuracy performance on the Chest Covid test set.

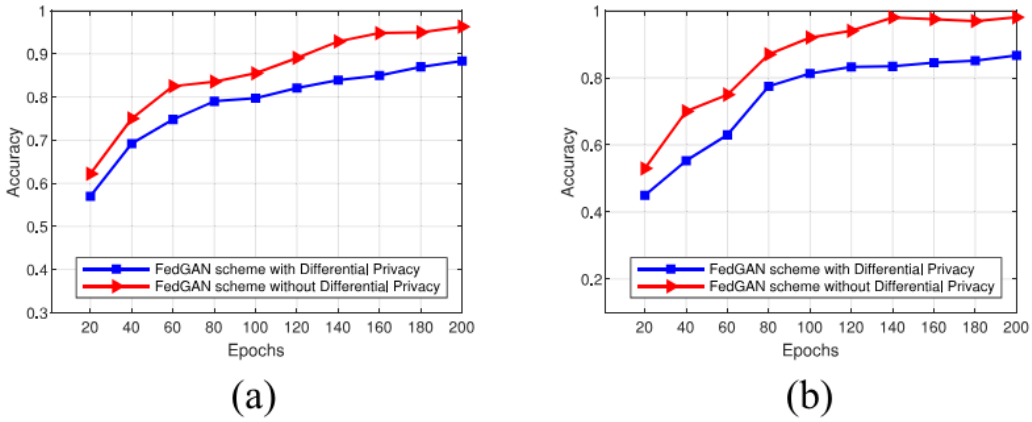

Fig : FL GAN with differential privacy enabled in terms of accuracy performance. Training with the Dark Covid data (a). Training using the Chest Covid data set (b).

7.2.3 Assessment of Comparative Privacy-Enabled FedGAN Efficiency

With set to 0.3, we examine our proposed system's accuracy and performance with differential privacy. Above figure illustrates this, even while differential privacy can provide COVID-19 data training some privacy, although its technique performs less well in terms of accuracy in both data sets. More research is still needed to determine how to strike a balance between data value (such training accuracy) and privacy preservation. Further we assess our scheme's effectiveness in terms of data usefulness when the privacy parameter is changed from 0.01 to 0.5, as shown by the F1 score. when seen in Figure 11, when rises, the degree of privacy falls, improving the usefulness of the data. For the Chest and Dark Covid data sets, this pattern is constant. Additionally, the simulation's outcome suggests that using the privacy parameter in
The effectiveness of FL training is significantly impacted by differentiable privacy settings.

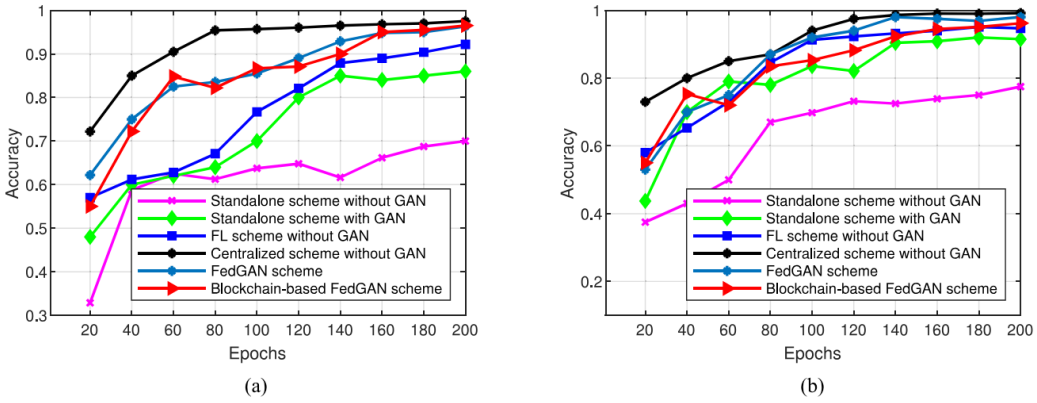

Fig : Analysing accuracy results in comparison. (a) Accuracy results on the DarkCOVID training data set. (b) Accuracy results on the ChestCOVID training dataset.

7.3 ASSESSMENTS OF FEDGAN PERFORMANCE USING BLOCKCHAIN

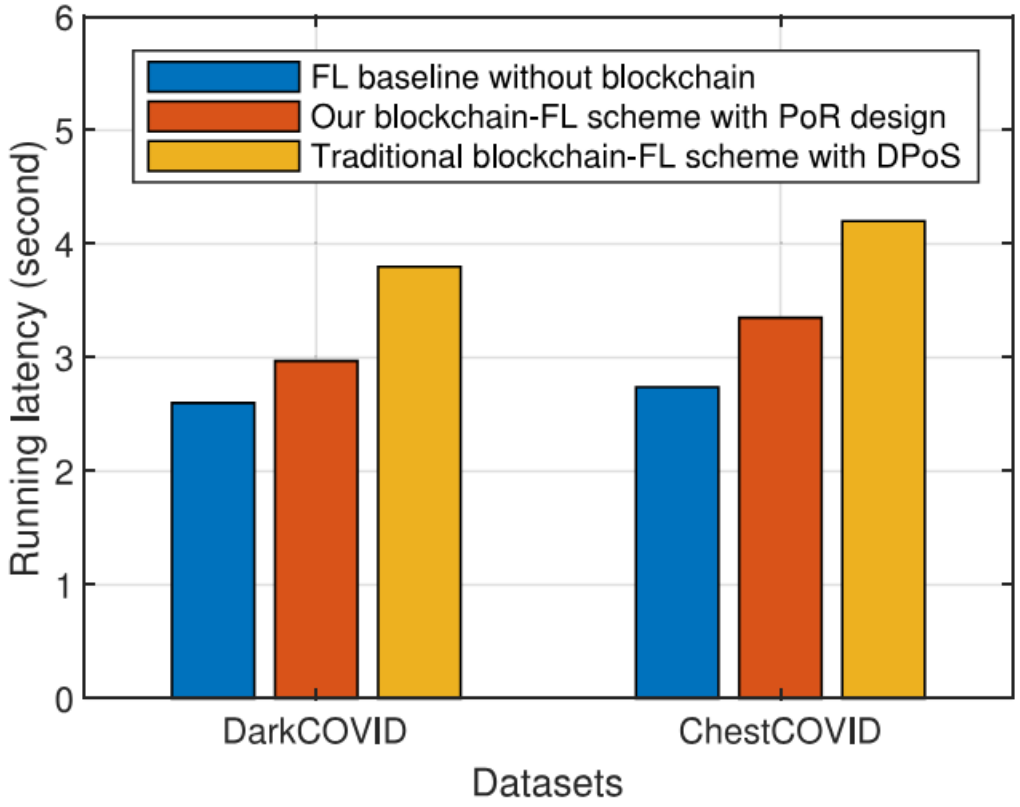

Fig : Comparison of running latency.

This portion will help to assess the effectiveness of the proposed Proof of Reputation consensus mechanism using numerical simulations and contrast its performance with the conventional Delegated Proof of Stake (DPoS) system by examining the block verification latency. We configure the system to process 10 transactions for each block and adjust the number of miners between 2 to 100. the criteria for mining are defined as : edge computing supply c_m range from 10^3 to 10^6 CPU cycles per second, the block data sizes B and B^{re} are 500 kB and 50 kB respectively, The pace of transmission in uplink r_m^{ul} is between 100 and 250 kbps, and The pace of

transmission in downlink r_m^{dl} is also between 100 and 250 kbps. Additionally, we set the parameter ξ to 0.5 and the mining time τ_m to 1000 milliseconds.

7.3.1 Block Verification for the Latency Performance

We assess the block mining delay in the blockchain network with 10 miners when we change the chunk of data size varies between 500 to 50 kb. our suggested mining plan thanks to our lightweight verification approach, produces a shorter verification delay than the conventional DPoS system. Specifically, our method exhibits significant benefits when data blocks are huge ($\geqslant$ 400 kB), whereas the DPoS approach takes a long time to validate such blocks.

7.3.2 Precision Outcomes

As result of examine and contrast our scheme's accuracy performance, which is based on blockchain technology, with other schemes that are similar. According to above figure simulation results, the blockchain-based With the FedGAN baseline scheme, the FedGAN system may attain competitive accuracy rates, particularly when trained on the DarkCOVID data set. This illustrates that whereas advertising a tall level of security for the combined information preparing, the integration of blockchain with a decentralized demonstrate conglomeration made conceivable by the blockchain agreement has no impact on the by and large preparing execution.

7.3.3 The effectiveness of the overall running latency

Following, we evaluate the contrasts in taken a toll between our PoR plan and the blockchain-based FedGAN plot in terms of the whole running idleness, which incorporates both the preparing and mining idleness at a worldwide preparing cycle. To guarantee unbiasedness, we utilize the immaculate FL methodology that fair contains the preparing inactivity and employments blockchain as the standard. Our proposed blockchain-based FedGAN plot may accomplish a decently comparable inactivity execution with the FL standard plot and spare a critical sum of working time when compared to the routine blockchain-based FedGAN plot with the DPoS, as appeared in Fig. 14 for both information sets. For occurrence, whereas preparing the DarkCOVID and ChestCOVID information sets, separately, our approach may cut the running time by 19.5% and 23.2% when compared to the ordinary plot utilizing DPoS. Our advanced agreement design, which decreases the mining inactivity during the conglomeration step and consequently brings down the whole preparing time, makes these discoveries conceivable.

Thought ought to be given to a number of issues and impediments in arrange to totally utilize FL-GAN in real-world healthcare systems. For occasion, guaranteeing compelling asset planning for ENs running GAN models is significant since mining and large-scale X-ray picture preparing call for considerable vitality and memory prerequisites. The failure of ENs to be spurred to participate in the FL-GAN prepare may give another trouble. In the event that there are no motivations or rewards, an edge hub might not be prepared to commit its assets to execute mining and prepare picture information sets. To guarantee the strength of the unified wellbeing information preparing, it is alluring to make fitting motivation components

to spur ENs from clinics to lock in within the FL-GAN prepare.

Chapter 8

FINAL THOUGHTS AND NEXT PROJECTS

8.1 CONCLUDING THOUGHTS

This paper presents FedGAN, an inventive approach for COVID-19 location that combines Unified Learning (FL) and Generative Antagonistic Systems (GAN) inside a dispersed restorative organize utilizing edge cloud computing. Our proposed strategy utilizes information increase through disseminated GANs and combined information preparing by means of FL, guaranteeing COVID-19 location without the got to share genuine information. To support protection in combined COVID-19 information preparing, we execute a differential security arrangement at each clinic institution. Along these lines, we show a novel blockchain-based FedGAN system for secure COVID-19 data analytics, decentralizing the FL prepare over clinic educate employing a one of a kind mining component. Hypothetical investigation and numerical reenactments illustrate that our approach essentially improves COVID-19 location execution, accomplishing tall precision rates and decreased running times compared to existing strategies.

8.2 FUTURE IDEAS FOR OUR PROJECT

In future endeavors, there's potential to amplify the proposed FL-blockchain show to other healthcare applications. For occasion, the

coordinates FL-blockchain system seem demonstrate important for unified human movement analytics, permitting wearable sensor gadgets to collaborate in preparing a shared human movement classification demonstrate. In such scenarios, blockchain innovation encourages the creation of a decentralized arrange of sensor gadgets for sharing demonstrate upgrades and planning preparing exercises, killing the require for centralized oversight.

REFERENCES

[1] X. Kong *et al.*, "Real-time mask identification for COVID-19: An edge computing-based deep learning framework," *IEEE Internet Things J.*, early access, Jan. 14, 2021, doi: 10.1109/JIOT.2021.3051844.

[2] M. Li *et al.*, "Scaling distributed machine learning with the parameter server," in *Proc. 12th USENIX Symp. Oper. Syst. Des. Implement. (OSDI)*, 2014, pp. 583–598.

[3] Q.-V. Pham *et al.*, "Artificial intelligence (AI) and big data for coronavirus (COVID-19) pandemic: A survey on the state-of-the-arts," *IEEE Access*, vol. 8, pp. 130820–130839, 2020.

[4] Y. Song *et al.*, "Deep learning enables accurate diagnosis of novel coronavirus (COVID-19) with CT images," *IEEE/ACM Trans. Comput. Biol. Bioinf.*, early access, Mar. 11, 2021, doi: 10.1109/TCBB.2021.3065361.

[5] K. H. Abdulkareem *et al.*, "Realizing an effective COVID-19 diagnosis system based on machine learning and IoT in smart hospital environment," *IEEE Internet Things J.*, early access, Jan. 11, 2020, doi: 10.1109/JIOT.2020.3050775.

[6] Y. Tai *et al.*, "Trustworthy and intelligent COVID-19 diagnostic IoMT through XR and deep learning," *IEEE Internet Things J.*, early access, Feb. 1, 2021, doi: 10.1109/JIOT.2021.3055804.

[7] T. Otzurk *et al.*, "Automated detection of COVID-19 cases using deep neural networks with X-ray images," *Comput. Biol. Med.*, vol. 121, Jun. 2020, art. no. 103792.

[8] Z. Pan *et al.*, "Recent progress on generative adversarial networks (GANs): A survey," *IEEE Access*, vol. 7, pp. 36322–36333, 2019.

[9] J. V. Kumar *et al.*, "Advanced machine learning-based analysis on COVID-19 data using generative adversarial networks," *Mater. Today Proc.*, to be published.

[10] C. Saez *et al.*, "Potential limitations in COVID-19 machine learning due to data source variability: A case study in the nCov-2019 dataset," *J. Amer. Med. Informat. Assoc.*, vol. 28, pp. 360–364, 2021.

[11] D. Liu *et al.*, "Federated learning for industrial Internet of Things in future industries," *IEEE Wireless Commun.*, early access, Aug. 6, 2021, doi: 10.1109/MWC.001.2000461.

[12] D. C. Nguyen *et al.*, "Federated learning for Internet of Things: A comprehensive survey," *IEEE Commun. Surveys Tuts.*, vol. 23, no. 2, pp. 1622–1686, 2nd Quart., 2021.

[13] J. Pang *et al.*, "Collaborative city digital twin for COVID-19 pandemic: A federated learning solution," Nov. 2020. [Online]. Available: arXiv:2011.02883.

[14] Q.-V. Pham *et al.*, "*EdgeHealth*: A decentralized architecture for edge-based IoMT networks using blockchain," *IEEE Internet Things J.*, vol. 8, no. 14, pp. 11745–11757, Jul. 2021.

[15] S. Motamed *et al.*, "RANDGAN: Randomized generative adversarial network for detection of COVID-19 in chest X-ray," Dec. 2021. [Online]. Available: arXiv:2012.08490.

[16] N. E. M. Khalifa *et al.*, "Detection of coronavirus (COVID-19) associated pneumonia based on generative adversarial networks and a fine-tuned deep transfer learning model using chest X-ray dataset," Apr. 2020. [Online]. Available: arXiv:2004.01184.

[17] M. Loey, F. Smarandache, and N. E. M. Khalifa, "Within the lack of chest COVID-19 X-ray dataset: A novel detection model based on GAN and deep transfer learning," *Symmetry*, vol. 12, no. 4, p. 651, Apr. 2020.

[18] H. Bao *et al.*, "COVID-GAN: Estimating human mobility responses to COVID-19 using generative adversarial networks," in *Proc. ACM 28th Int. Conf. Advances Geographic Inf. Syst.*, Nov. 2020, pp. 273–282.

[19] H. Liu *et al.*, "Dynamic fusion-based federated learning for COVID-19 detection," *IEEE Internet Things J.*, early access, Feb. 4, 2021, doi: 10.1109/JIOT.2021.3056185.

[20] Y. Zhang *et al.*, "Self-supervised learning for COVID-19 detection based on multi-national data from China, Italy, Japan," *Med. Image Anal.*, vol. 70, May 2021, art. no. 101992.

[21] J. Ouyang *et al.*, "Crowdsourced deep learning for detecting COVID-19 lung abnormalities in CT: A privacy-preserving multinational validation study," *IEEE J. Biomed. Health Inform.*, vol. 4, no. 1, p. 60, Dec. 2021.

[22] I. Feixi *et al.*, "Federated deep learning for COVID-19 screening from chest X-ray images," *Appl. Soft Comput. J.*, vol. 106, Jul. 2021, art. no. 107330.

[23] H. Liu *et al.*, "Experiments of federated learning for COVID-19 chest X-ray," Jul. 2020. [Online]. Available: arXiv:2007.05592.

[24] R. Kumar *et al.*, "Blockchain-federated-learning and deep learning models for COVID-19 detection using CT imaging," *IEEE Access*, vol. 8, pp. 101929–101949, Jun. 2020.

[25] A. I. Ridwan and H. T. Mouftah, "Preventing and controlling COVID-19 using blockchain-assisted AI-enabled networks," *IEEE Netw.*, vol. 35, no. 3, pp. 34–41, May 2021.

[26] S. Garg *et al.*, "Blockchain orchestrated machine learning for secure and transparent election system: An electronic health record perspective," in *Proc. IEEE Int. Conf. Blockchain (Blockchain)*, Nov. 2020, pp. 550–555.

[27] M. Rahman *et al.*, "Blockchain and federated learning-based structures for secure electronic health records sharing," *IEEE Trans. Ind. Inform.*, vol. 17, no. 8, pp. 2964–2973, Jul. 2020.

[28] M. M. Rahman *et al.*, "Explainable AI for healthcare: A survey, research directions and challenges," *Comput. Biol. Med.*, vol. 21, pp. 102087–102094, Apr. 2021.

[29] M. Rahman *et al.*, "Federated learning and blockchain-based enhanced framework for privacy preservation in IoMT," *IEEE Access*, vol. 9, pp. 30551–30568, 2021.

[30] M. Shen *et al.*, "Exploiting unintended property leakage in blockchain-assisted federated learning for intelligent edge computing," *IEEE Internet Things J.*, vol. 8, no. 4, pp. 2265–2275, Feb. 2021.

[31] I. J. Goodfellow *et al.*, "Generative adversarial nets," in *Proc. Adv. Neural Inf. Process. Syst.*, vol. 27, 2014, pp. 2672–2680.

[32] D. C. Nguyen *et al.*, "Blockchain and AI-enabled solutions to combat coronavirus (COVID-19)-like epidemics: A survey," *IEEE Access*, vol. 9, pp. 95730–95753, 2021.

[33] D. C. Nguyen *et al.*, "Federated learning meets blockchain in edge computing: Opportunities and challenges," *IEEE Internet Things J.*, vol. 8, no. 6, pp. 12806–12825, Aug. 2021.

[34] T. Zhou, X. Li, and H. Zhao, "DLatice: A permission-less blockchain based on DPoS-Ba-DAG consensus for data tokenization," *IEEE Access*, vol. 7, pp. 39273–39287, 2019.

[35] I. D. Apostolopoulos and T. A. Mpesiana, "COVID-19: Automatic detection from X-ray images utilizing transfer learning with convolutional neural networks," *Phys. Eng. Sci. Med.*, vol. 43, no. 2, pp. 635–640, Jun. 2020.

[36] J. Kang *et al.*, "Toward secure blockchain-enabled Internet of Vehicles: Optimizing consensus management using reputation and contract theory," *IEEE Trans. Veh. Technol.*, vol. 68, no. 3, pp. 2906–2920, Mar. 2019.

[37] P. Afshar *et al.*, "COVID-CAPS: A capsule network-based framework for identification of COVID-19 cases from X-ray images," *Pattern Recognit. Lett.*, vol. 138, pp. 638–643, Oct. 2020.

[38] J. Long, E. Shelhamer, and T. Darrell, "Fully convolutional networks for semantic segmentation," in *Proc. IEEE Conf. Comput. Vis. Pattern Recognit.*, 2015, pp. 3431–3440.